ELSEVIER

Physica C 341–348 (2000) 2193–2196

PHYSICA C

www.elsevier.nl/locate/physc

Superfluid and normal-fluid densities in the high-T_c superconductors

D.B. Tanner[a], F. Gao[a], K. Kamarás[a], H.L. Liu[a], M.A. Quijada[a], D.B. Romero[a], Y-D. Yoon[a], A. Zibold[a], H. Berger[b], G. Margaritondo[b], L. Forró[b], R.J. Kelly[c], M. Onellion[c], G. Cao[d], J.E. Crow[d], Beom-Hoan O[e], J.T. Markert[e], J.P. Rice[f], D.M. Ginsberg[f], and Th. Wolf[g]

[a]University of Florida; [b]École Polytechnique Fédéral de Lausanne; [c]University of Wisconsin; [d]National High Magnetic Field Laboratory; [e]University of Texas; [f]University of Illinois; [g]Forschungszentrum Karlsruhe

In clean metallic superconductors, 100% of the mobile carriers participate in the condensate, so that the London penetration depth (which measures the electromagnetic screening by the superconductor) indicates charge densities comparable to those inferred from the free-carrier plasma frequency. In the cuprates, this is not the case, even though penetration depth measurements have shown a good correlation between superfluid density and superconducting transition temperature in the underdoped-to-optimally-doped part of the phase diagram. Optical measurements, which permit independent determination of the total doping-induced spectral weight and the superfluid density, show that in optimally doped materials only about 20% of the doping-induced spectral weight joins the superfluid. The rest remains in finite-frequency, midinfrared absorption. In underdoped materials, the superfluid fraction is even smaller. This result implies extremely strong coupling for these superconductors.

1. INTRODUCTION

When the cuprate superconductors are doped, spectral weight or oscillator strength is transferred out of the 1.5–2 eV charge-transfer transition into the low-energy regime.[1–4] When the material is superconducting, some of this low-energy spectral weight appears in a zero-frequency delta function, while the remainder is at finite frequency. (The delta function represents the infinite dc conductivity of the superfluid; via the Kramers-Kronig relations it leads to a finite-frequency inductive response and electromagnetic penetration depth.)

Infrared measurements of these spectral weights on a variety of cuprates are described here. The results show that a relatively-small fraction ($\sim$ 20%) of the spectral weight appears in the zero-frequency delta function. In this, the cuprates differ from clean metallic superconductors, where essentially every conduction electron participates in the $T = 0$ superfluid.[5,6] In the latter materials, the penetration depth, corrected for nonlocal effects, gives about the same electron density as the free-carrier optical plasma frequency ω_p, i. e., $\Lambda_L^{-2} = 4\pi n_s e^2/cm^* = \omega_{ps}/c$ with $\omega_{ps} \approx \omega_p$. Here, Λ_L is the London value for the penetration depth, n_s is the density of superconducting electrons and m^* their effective mass.

2. OPTICAL TECHNIQUES

We measured the near-normal-incidence, polarized reflectance $\mathscr{R}$ using a Bruker IFS-113v Fourier-transform spectrometer in the far-infrared and midinfrared region (80–4000 cm^{-1}) and a modified Perkin-Elmer 16U grating spectrometer in the near-infrared and ultraviolet (2000–33,000 cm^{-1}). We used wire grid polarizers in the far–midinfrared and dichroic polarizers in the

0921-4534/00/$ – see front matter
PII S0921-4534(00)00970-9

near infrared–ultraviolet. Low-temperature measurements (10–300 K) employed a continuous-flow cryostat.

We measured spectra at each temperature for both the sample and for a reference Al mirror. Their ratio gives a preliminary reflectance of the sample. After completing these measurements at each temperature for each polarization, we measured a final room temperature spectrum, coated the sample with 2000 Å of Al, and remeasured this coated surface. The ratio of the spectrum from the uncoated sample to the reflectance of the coated surface was multiplied by the known reflectance of Al to give the most accurate result for the room-temperature reflectance. This result was then used to correct the reflectance data measured at other temperatures by comparing the individual room-temperature spectra taken in the two separate runs. This procedure compensates for any misalignment between the sample and the mirror used as a temporary reference before the sample was coated, corrects for interference in the cryostat window, and, most importantly, provides a reference surface of the same size and profile as the actual sample.

The uncertainties in the absolute value of the reflectance are in the order of $\pm 1\%$. This uncertainty is in good agreement with the reproducibility found from the measurements of different samples[7] and leads to an uncertainty in the conductivity which varies with frequency, equal to $\pm 1\% \cdot \mathscr{R}(\omega)/\{1 - [\mathscr{R}(\omega)]^2\}$.

3. KRAMERS-KRONIG ANALYSIS

We used Kramers-Kronig transformation of the reflectance data[8] to obtain the optical conductivity and other optical "constants." The low- and high-frequency extrapolations were done in the following way. We extended the low-frequency data using a Drude-Lorentz model, dominated at the low frequencies by the free-carrier (Drude) form. In the superconducting state, the reflectance is expected to be unity for frequencies close to zero, and we used the same Drude-Lorentz model, but with the Drude scattering rate set to zero. We used data from the literature, where available, to extend the high-frequency end, and then used $\mathscr{R}(\omega) \sim \omega^{-s}$ up to a crossover frequency ω_f and $\mathscr{R}(\omega) \sim \omega^{-4}$ (as appropriate for free electrons) thereafter. The exponent s is a number that typically lies between 0 and 4; we used $s \sim 1$. The crossover frequency was chosen to be $\sim 1,000,000\,\mathrm{cm}^{-1}$ (125 eV) We observed some dependence of the results on the choice of s and ω_f for frequencies close to the highest frequencies. For frequencies below $20{,}000\,\mathrm{cm}^{-1}$, however, the effects of this choice were insignificant.

4. OPTICAL CONDUCTIVITY

The optical conductivity at two temperatures for the a-axis of a $Bi_2Sr_2CaCu_2O_8$ single crystal is shown in Fig. 1. In the normal state (100 K), the low-frequency optical conductivity extrapolates reasonably well to the dc conductivity. The temperature dependence[7,9] agrees with the T-linear resistivity and there is a characteristic narrowing of this far-infrared portion of the spectrum. In contrast, $\sigma_1(\omega)$ does not show much temperature variation at high frequencies. Below

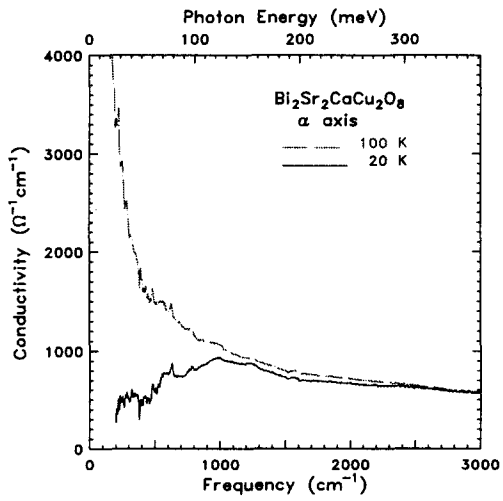

Fig. 1. Optical conductivity for the a-axis of $Bi_2Sr_2CaCu_2O_8$.

T_c, the low-frequency conductivity is considerably reduced. The "missing area" in the far-infrared conductivity appears as the zero-frequency delta-function response of the superfluid.

5. SUM RULE ANALYSIS

Infrared spectroscopy may be used to estimate the doping-induced spectral weight, using the partial sum rule for the optical conductivity.[8]

$$N_{eff}(\omega)\frac{m}{m^*} = \frac{2mV_{\text{cell}}}{\pi e^2}\int_0^{\omega}\sigma_1(\omega')d\omega' \qquad (1)$$

where e and m are the free-electron charge and mass respectively, m^* the effective mass, and V_{cell} the volume occupied by one formula unit. For simplicity, we will take $m^* = m$ in this section and consider $N_{eff}(\omega)$ to represent the effective number of carriers per formula unit participating in optical transitions below frequency ω. Figure 2 shows as the upper (solid) curves N_{eff} for the a-axis of a single-domain $Bi_2Sr_2CaCu_2O_8$ crystal at $T = 100$ K.[9] The curve rises, begins to flatten out, and then increases slope at the onset of the charge-transfer band. The short dashed line is obtained by subtracting from $\sigma_1(\omega)$ the contributions of the charge-transfer and higher-lying bands (obtained by a fit of the data to a Drude-Lorentz model) before integration. The value at which the 100 K dashed line saturates is a good estimate of N_{eff}.

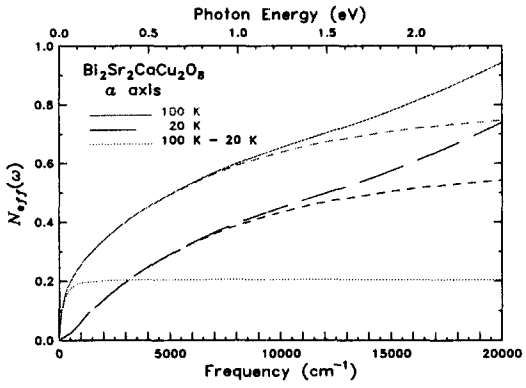

Fig. 2. Partial sum rule for the a-axis of $Bi_2Sr_2CaCu_2O_8$.

To estimate the superfluid density, N_s, one may evaluate $N_{eff}(\omega)$ for $T < T_c$. The data table for $\sigma_1(\omega)$ naturally omits the zero-frequency infinite dc conductivity; thus the numerical integral misses the delta-function contribution, and the "missing area" in $N_{eff}(\omega)$ below T_c gives the superfluid density. Figure 2 shows (as the long dashed curves) N_{eff} at 20 K for the a-axis of a single-domain $Bi_2Sr_2CaCu_2O_8$ crystal.[9] The 20 K data are nearly parallel to the 100 K data; the dotted line is the difference between them, and is an estimate of N_s.

6. DISCUSSION

Figure 3 shows the results for single crystals of a number of materials. The left panel shows a "Uemura plot,"[10] displaying T_c as a function of the ab-plane superfluid density. (The superfluid density is expressed as carriers per copper atom in order to allow for the differing number of Cu layers and differing interlayer spacing in the materials studied; however a plot as a function of 3-dimensional carrier density looks very similar.[11]) The typical linear increase of T_c with superfluid density is clearly seen.

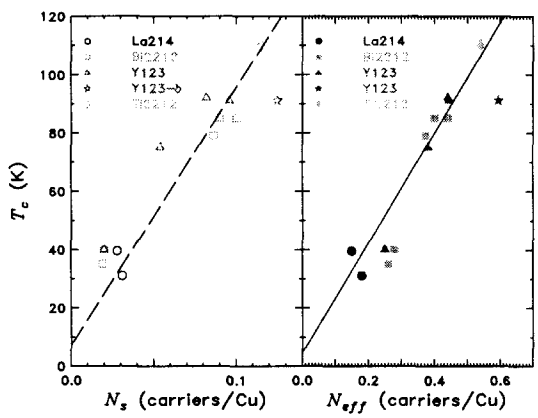

Fig. 3. Left panel: $T_c$as a function of the superfluid density. Right panel: T_c as a function of the total doping-induced spectral weight. The lines are least square fits to the data for optimally doped crystals.

The right panel shows T_c as a function of the *total* doping-induced carrier density, N_{eff}. A linear increase of T_c with total carrier density is clearly seen. The difference between the two panels is that the horizontal scale of the right-hand plot is five times that of the left-hand plot, implying that only about 1/5 of the doped-in carriers join the superfluid. This ratio holds quite closely for all optimally-doped materials, from T_c = 40 K $La_2CuO_{4+\delta}$ to T_c = 110 K $Tl_2Ba_2CaCu_2O_8$. It even works reasonably well for the b axis of $YBa_2Cu_3O_7$ (represented by the stars in the figure) for which we have assumed 3 coppers per formula unit. For underdoped materials the ratio N_s/N_{eff} becomes smaller and smaller as the doping level decreases from the optimum amount.

We interpret this result as evidence for extremely strong coupling in these materials. The electrons in the superconducting condensate have an enhanced effective mass on account of the interactions among them. These strength of these interactions is described by a dimensionless parameter, λ, which also determines the mass enhancement: $m^* = (1+\lambda)m$, where m is the band mass. The oscillator strength of the condensate's delta-function response is decreased by this same factor, so that $(\frac{m}{m^*})N_{eff}$ becomes smaller as λ becomes larger. At the same time, the interaction moves oscillator strength to finite frequencies via the Holstein effect,[12] so that the sum rule is satisfied. The reduction of the superfluid density by a factor of 5 which we observe implies therefore that $\lambda = 4$, an extremely strong- coupling value. Note that this result is not consistent with the value $\lambda = 0.3$ inferred from the temperature or frequency dependence of $1/\tau(\omega, T)$.[9,13,14] The resolution of this conflict is not obvious at the present time.

7. ACKNOWLEDGMENTS

We acknowledge many discussions with P.J. Hirschfeld. Work at Florida was supported by the NSF—Solid State Physics—through grant number DMR-9705108. Research at the EPFL has received support from the Swiss National Science Foundation, at Wisconsin from the DOE, at the National High Magnetic Field Laboratory from NSF Cooperative Agreement No. DMR-9527035 and the State of Florida, at Texas from NSF Grant DMR-9158089, and at Illinois from NSF Grant DMR-9120000 through the Science and Technology Center for Superconductivity.

REFERENCES

1. S.L. Cooper, G.A. Thomas, J. Orenstein, D.H. Rapkine A.J. Millis, S.-W. Cheong, A.S. Cooper, and Z. Fisk, *Phys. Rev. B* **41** (1990) 11605.
2. S. Uchida, T. Ido, H. Takagi, T. Arima, Y. Tokura, and S. Tajima, *Phys. Rev. B* **43** (1991) 7942.
3. M.B.J. Meinders, H. Eskes and G.A. Sawatzky, *Phys. Rev. B* **48** (1993) 3916.
4. H. Eskes, A.M. Oles, M.B.J. Meinders, and W. Stephan, *Phys. Rev. B* **50** (1994) 17980.
5. A.B. Pippard, *Proc. Roy. Soc. (London)* **A216** (1953) 547.
6. M. Tinkham, *Introduction to Superconductivity, Second Edition*, (McGraw-Hill, New York, 1996).
7. M.A. Quijada, D.B. Tanner, R.J. Kelley and M. Onellion, *Z. Phys. B* **94** (1994) 255.
8. Frederick Wooten, *Optical Properties of Solids* (Academic Press, New York, 1972).
9. M.A. Quijada, D.B. Tanner, R.J. Kelley, M. Onellion, and H. Berger, *Phys. Rev. B* **60** (1999) 14000.
10. Y.J. Uemura, L.P. Le, G.M. Luke, B.J. Sternlieb, W.D. Wu, J.H. Brewer, T.M. Riseman, C.L. Seaman, M.B. Maple, M. Ishikawa, D.G. Hinks, J.D. Jorgensen, G. Saito, and H. Yamochi, *Phys. Rev. Lett.* **66** (1991) 2665.
11. H.L. Liu, M.A. Quijada, A. Zibold, Y.-D. Yoon, D.B. Tanner, G. Cao, J.E. Crow, H. Berger, G. Margaritondo, L. Forró, Beom-Hoan O, J.T. Markert, R.J. Kelly, and M. Onellion, *J. Phys.: Condens. Matter* **11** (1999) 239.
12. T. Holstein, *Phys. Rev.* **96** (1954) 535.
13. S.L. Cooper, A.L. Kotz, M.A. Karlow, M.V. Klein, W.C. Lee, J. Giapintzakis, and D.M. Ginsberg, *Phys. Rev. B* **45** (1992) 2549.
14. D.B. Romero, C.D. Porter, D.B. Tanner, L. Forro, D. Mandrus, L. Mihaly, G.L. Carr, and G.P. Williams, *Solid State Commun.* **82** (1992) 183.